

MORPHOLOGICAL AND MICROSTRUCTURAL FEATURES OF Al-BASED ALLOYED POWDERS FOR POWDER-METALLURGY APPLICATIONS

MORFOLOŠKE IN MIKROSTRUKTURNE ZNAČILNOSTI KOVINSKIH PRAHOV NA OSNOVI ALUMINIJA ZA IZDELAVO IZDELKOV PO POSTOPKIH METALURGIJE PRAHOV

**Borivoj Šuštaršič¹, Irena Paulin¹, Matjaž Godec¹, Srečko Glodež², Marko Šori²,
Jože Flašker², Albert Korošec³, Stanko Kores³, Goran Abramovič³**

¹Institute of Metals and Technology, Lepi pot 11, 1000 Ljubljana, Slovenia

²University of Maribor, FNM, Koroška cesta 160, 2000 Maribor, Slovenia

³Talum, Factory of Aluminium, Tovarniška cesta 10, 2325 Kidričevo, Slovenia
borivoj.sustarsic@imt.si

Prejem rokopisa – received: 2013-12-16; sprejem za objavo – accepted for publication: 2014-02-20

Besides advanced nano steels, polymers and ceramics, recently also light metals, i.e., Al, Mg and Ti based materials, have been recognized as future materials for different kinds of advanced applications. Al and its alloys have an acceptable price, excellent corrosive resistance, good mechanical and other physical properties. Therefore, they are also used in the powder-metallurgy (P/M) field. The P/M technology of Al materials is very demanding and has its own specifics compared to the sintering technology of iron and steel. A relatively large quantity of Al-based alloy powder is formed during the sand blasting of slugs and discs in the Talum Al factory, Kidričevo, Slovenia. Therefore, we analysed and investigated its practical usability for a production of advanced products using P/M technology. The formed Al-based powder was compared with the commercially available Al-based powders that are generally used for conventional sintering technology. In the first part of this paper we explain which types of Al-based powders are used for the production of sintered parts, what the required parameters are and why we considered them. Then, the results of theoretical thermodynamic analyses and investigations of the morphological and microstructural characteristics of the selected commercial Al-based powders are given, as well as their comparison with the Al powder formed during the sand blasting and its potential for P/M applications.

Keywords: Al-based alloy powders, morphology and microstructure, LM and SEM/EDS characterisation

Postopki metalurgije prahov (P/M) so med najučinkovitejšimi tehnologijami za velikoserijsko izdelavo majhnih izdelkov kompliciranih oblik. Med vsemi P/M-postopki je najbolj uveljavljen t. i. konvencionalni sinter postopek. Z njim izdelujemo predvsem izdelke na osnovi železa. To so sintrani jekleni zobniki, zaklepi, puše, porozni filtri, ležaji, kakor tudi drugi strojni ali konstrukcijski elementi strojev in naprav. Zelo popularni so tudi sintrani izdelki na osnovi Fe za mehko- in trdomagnetne aktuatorje in senzorje. Največji odjemalec sintranih izdelkov je avtomobilska industrija. Najdemo pa jih tudi v pohištveni industriji, beli tehniki, precizni mehaniki, v izdelkih za šport in razvedrilo, kakor tudi za zelo zahtevne letalske, vojaške, vesoljske in druge aplikacije. Na vseh teh področjih se v novejšem času uveljavljajo poleg polimerov in keramike tudi lažji kovinski materiali, kot so zlitine na osnovi Al, Mg in Ti. Aluminij oz. njegove zlitine se zaradi svojih odličnih mehanskih, korozijskih in drugih fizikalnih lastnosti uveljavljajo tudi na področju P/M-tehnologij. Ta tehnologija Al-materialov je zelo zahtevna, ima svoje specifičnosti in se precej razlikuje od sinter tehnologije Fe in jekla. V tovarni aluminija Talum kot stranski produkt peskanja rondelic nastaja legiran Al-prah. Zato smo analizirali njegovo praktično uporabnost in možnosti izdelave zahtevnih izdelkov s P/M-postopkom. Nastajajoči Al-prah smo primerjali s komercialno dosegljivimi Al-prahovi, ki se standardno uporabljajo za konvencionalno sinter tehnologijo Al. V prispevku predstavljamo tudi, kakšni prahovi so uporabni za izdelavo sintranih izdelkov, kaj se od njih zahteva in zakaj. Predstavljeni so rezultati teoretičnih termodinamskih analiz in raziskav s poudarkom na morfoloških in mikrostrukturnih značilnostih komercialno dosegljivih prahov na osnovi Al in primerjava z Al-prahom peskanja. Ocenili smo tudi njegovo uporabnost za izdelavo izdelkov s P/M-tehnologijo.

Ključne besede: kovinski prahovi zlitine na osnovi Al, morfologija in mikrostruktura, preiskave s svetlobnim in elektronskim mikroskopom

1 INTRODUCTION

The powder-metallurgy process (P/M) is one of the most efficient technologies for a mass production of small complex functional and structural products. Conventional sintering technology (**Figure 1**) is the most convenient and popular technology among all the P/M processes. A fine metal-powder mixture is first automatic die compacted (ADC) into the final shape of the product with automatic mechanical or hydraulic presses and then sintered in a protective atmosphere at the temperatures between approximately 0.8 and 0.9 of the melting point

of the metal powder. The result of this procedure is a partly porous or completely dense metal product that can be additionally improved with heat and/or mechanical treatments. Iron- and steel-based P/M products are mainly produced with this procedure. These are sintered steel gears, spurs, locking mechanisms, porous filters, sliding bearings, as well as other machine and structural elements. Sintered soft/hard magnetic actuators and sensors are also very popular. The automotive industry is the most important end user of sintered parts. However, small complex sintered parts can be frequently used also in the furniture and household industry, precision mecha-

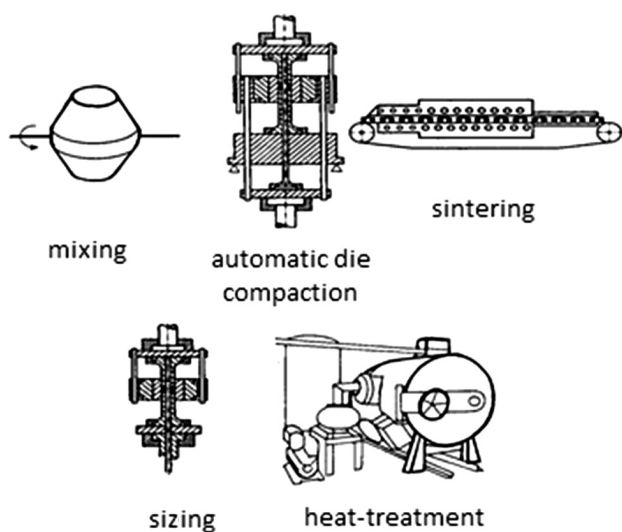


Figure 1: Schematic presentation of conventional sintering process
Slika 1: Shematski prikaz konvencionalnega postopka sintranja

tics, the articles for leisure, recreation and sports, etc. High-alloyed sintered metal parts can also be used for very demanding marine, aeronautic, military and space applications.¹

Besides advanced nano steels, polymers and ceramics, recently also light metals, i.e., Al, Mg and Ti based materials, have been recognized as future materials for different kinds of advanced applications.^{2,3} Aluminium and its alloys have an acceptable price, excellent corrosive resistance, good mechanical and other physical properties (non-magnetic, excellent thermal and electrical conductivity, etc.). Therefore, they are also used in the P/M technology field (Figure 2).⁴

However, the P/M technology of Al materials is very demanding and has its own specifics compared to the sintering technology of iron and steel.^{5,6} The Al-based alloyed powders, appropriate for a sintering procedure (powder metallurgy, P/M) contain the alloying elements (Cu, Zn, Mg, etc.) with a high solid solubility in Al, enabling reaction and liquid-phase sintering, respectively. The high solid solubility of these elements is also important for an additional improvement of mechanical properties, enabling precipitation hardening during a heat treatment. Generally, Al powders are surface oxidised because of the high affinity of Al to oxygen.



Figure 2: Some small complex Al-based sintered parts⁴

Slika 2: Nekaj majhnih in kompliciranih sintranih izdelkov na osnovi Al⁴

Besides, these types of powders also contain approximately the mass fraction 1.5 % of polymeric lubricant (wax) that reduces the friction at die walls, while the powders are being ADC into the final compact shapes of the products. This lubricant has to be removed slowly during the first stage of sintering in order to prevent deformations and cracking of the product. Therefore, its sintering is very complex. Generally, these types of powders are sintered in pure nitrogen (N₂, 5.9) with a low dew point (below -40 °C). The optimum sintering conditions are commonly determined on the basis of light (LM) and scanning electron microscopy (SEM) combined with a micro-chemical analysis based on the measurement of the dispersed kinetic energy of X-rays (energy dispersive X-ray spectrometer, EDS). The investigation can also be completed very successively with hot microscopy, as well as with differential scanning calorimetry and thermogravimetry (DSC/TG).⁷

A relatively large quantity of Al-based alloy powder is formed as a bypass product during the sand blasting of slugs (Figure 3) and discs in the Talum Al factory, Kidričevo, Slovenia.⁸ Therefore, we analysed and investigated its practical usability for the production of the advanced products made with the P/M technology. The formed Al-based powder was compared with the commercially available Al-based powders that are generally used for conventional sintering technology. In the first part of this paper we explain which types of Al-based powders are generally used for the production of sintered parts, what the required parameters are and why we con-



Figure 3: Slugs produced in the Talum Al factory used as semi-products in the production of tubes and containers in the pharmaceutical, food and cosmetic industries⁸

Slika 3: Rondelice, izdelane v tovarni aluminija Talum, ki se uporabljajo kot polproizvod v proizvodnji tub in posodic za kozmetiko ter v farmacevtski in prehrabeni industriji⁸

sidered them. Then, the results of the theoretical thermodynamic analyses and investigations of the morphological and microstructural characteristics of the selected commercial Al-based powders are presented and their comparison with the Al powder formed during the sand blasting, together with its potential for P/M applications, are given. Henceforth, this Al powder will be designated as the SB powder.

2 CHEMICAL AND THERMODYNAMIC CHARACTERISTICS OF THE Al POWDERS

In the frame of the present project,⁹ three commercial Al-based powders (Alumix 123, 231 and 432) appropriate for the sintering technology were purchased at Ecka Granules, Germany.¹⁰ Henceforth, these three commercial alloys will be designated as alloys *A*, *B* and *C*. The powder producer has already provided some recommendations for the sintering of these alloy powders. However, in some cases these data are not enough to get all the necessary information for their comparison with the SB powder. Therefore, first, a complete theoretical thermodynamic analysis as well as morphological and microstructural characterisations of the selected commercial powders were performed.

Table 1 shows the nominal and actual chemical compositions of the investigated powders. One can notice that the chemical compositions of these alloys are very simple. Wrought Al alloys (extruded, forged) of similar types usually have more complex compositions with additional amounts of alloying elements (Cr, Ti, Zr, V, etc.) and, generally, lower amounts of impurities and oxygen. The chemical composition of the SB powder differs significantly from the commercial alloys. It has much higher amounts of Cu, Fe and Mn but lower amounts of Mg and Zn. Only its Si content is comparable with the amount in alloy *A*, but it does not contain Zn. In view of the above, it is practically impossible to dilute the SB powder with additional corrections (by adding appropriate amounts of Al and other elements) in order to prepare an alloy similar to the one of the commercial alloys given in **Table 1**.

In the first phase of the investigation, to understand the sintering process, it is necessary to be acquainted at

least with the experimentally determined binary-phase diagrams of Al with the basic alloying elements (Al-Cu, Al-Si, Al-Mg, Al-Zn) and with their mutual congruency (Si-Cu, Si-Mg, Mg-Cu, Mg-Zn).¹¹ Such information gives us the appropriate data about the temperature solid-state solubility of an individual alloying element in Al, the basic temperature stability of the formed binary phases and the melting points. Certain ternary-phase diagrams with known multi-component intermetallic phases are also available in the professional, but relatively expensive, databases.¹²

From the considerably complex (eutectic-peritectic/peritectoid) Al-Cu equilibrium binary-phase diagram¹¹ one can see that the solid solubility of Cu in Al is maximal at 548 °C (approximately 5.7 %). The eutectic reaction ($L \Rightarrow \alpha\text{Al} + \theta$) is carried out at 67 % of Al. All our three commercial alloys have such Cu amounts that all the Cu is soluble in the fcc αAl solid solution during the sintering. At the same time, it follows from the Cu-Si binary diagram that Cu has a good solubility for Si, while Cu is not soluble in Si.

The Al-Si equilibrium binary-phase diagram is of the pure eutectic type.¹¹ The eutectic ($\alpha\text{Al} + \text{Si}$) is formed at 577 °C and approximately 87.5 % Al. The solid solubility of Si in Al is small. It is maximal at the eutectic temperature (1.56 %). One can see in **Table 1** that the composition of alloy *A* enables practically all the Si to be soluble in the αAl solid solution during the sintering. On the other hand, alloy *B* has a much higher amount of Si, and, therefore, one can expect the presence of hard Si crystals in the metal matrix, enabling a high hardness and good wear resistance of this alloy. The third alloy, alloy *C*, does not contain Si.

The Al-Mg equilibrium binary-phase diagram is of the double eutectic type.¹¹ The solid solubilities of Mg in Al and Al in Mg are good. At the eutectic temperatures of 450 °C and 437 °C the solid solubilities are approximately 17 % of Mg and approximately 12 % of Al, respectively. Mg is present as an alloying element in all three commercial alloys and one can expect that almost all of it is dissolved in the αAl solid solution during the sintering. Why almost? Because a certain part of an

Table 1: Nominal and actual average bulk chemical compositions of the investigated powders

Tabela 1: Nazivna in dejanska povprečna kemijska sestava preiskovanih prahov

Chemical composition		Cu	Si	Mg	Zn	Al	Other elements	Remark
Name		mass fractions, w/%						
Alloy <i>A</i>	nominal ¹⁰	4.2–4.8	0.5–0.7	0.4–0.6	–	bal.	–	type 2xxx (2014)
	actual	4.5	0.62	0.48	–	n. d.*	0.08 Fe	
Alloy <i>B</i>	nominal ¹⁰	2.4–2.8	14–16	0.5–0.8	–	bal.	–	Hypereutectic high Si (wear resistant)
	actual	2.7	15.0	0.58	–	n. d.	–	
Alloy <i>C</i>	nominal ¹⁰	1.4–1.8	–	2.2–2.8	5.0–5.8	bal.	–	type 7xxx (7075)
	actual	1.6	–	2.4	5.8	n. d.	0.29 Sn	
SB powder	actual	7.74	0.83	0.1	1.57	87.0	1.6 Fe 0.48 Mn	Bypass product of sand blasting

* n. d. not determined

alloying element is also present in the liquid phase during the liquid-phase sintering.

From the considerably complex (eutectic-eutectoid) Al-Zn equilibrium binary-phase diagram¹¹ one can see that Zn has a large solid solubility in Al. The maximum solubility at 382 °C is 83 %. At approximately 340 °C a spinodal decomposition occurs ($\alpha \Rightarrow \alpha + \alpha'$) followed (at the lower temperatures) by the phase transformations of $\alpha + \gamma$ and $\alpha + \beta$. The Zn alloying element is present only in commercial alloy *C*. This alloy also has a small amount of tin (Sn) that has a very low melting point (232 °C) and a good solubility in solid Cu (bronzes) and in Mg, but it is not soluble in Zn and Al.

However, recent modern CALPHAD-based (Calculation of Phase Diagrams)¹³ computer tools (ThermoCalc, DICTRA, etc.)¹³⁻¹⁵ enable a faster and more reliable insight into complex multi-component systems. The thermodynamic analysis of alloy *A* with ThermoCalc¹⁵ shows (**Figure 4**) that it mostly contains the solid crystals of the α Al phase (from room temperature up to 637.81 °C) and intermetallic θ phase (Al₂Cu) up to 500.96 °C. The first liquid appears at 525.04 °C. The theory also predicts a formation of small amounts of the intermetallic phases of Al₅Cu₂Mg₈Si₆ (up to 500 °C), Al₇Cu₂M (M = Fe, up to 565.04 °C), β AlFeSi (up to 223.2 °C) and Si to approximately 396 °C. The exact chemical composition of each individual phase can also be determined for the whole temperature region. A two-phase region (L + α Al) exists between 525.04 °C and 637.81 °C. At the beginning of this temperature region (somewhere between 570 °C and 600 °C) where a small quantity of liquid is already formed, there is the appropriate optimum (maximum) sintering temperature. The powder producer recommends a sintering temperature between 590 °C and 600 °C for 20 min, which is in good agreement with the theoretical thermodynamic calculation.

Unfortunately, the limited scope of this article does not allow us to show all the results of the performed thermodynamic analyses of the investigated alloys. There-

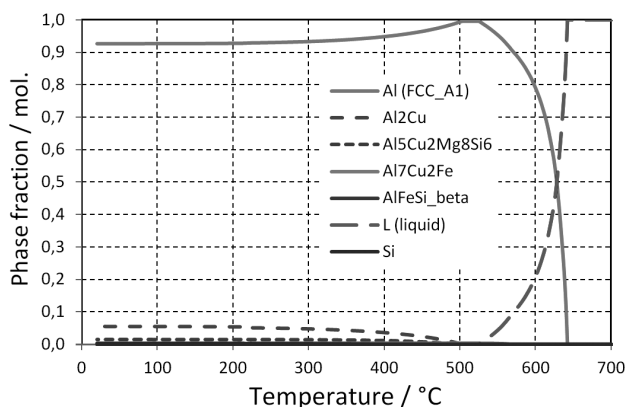


Figure 4: Theoretical equilibrium thermodynamic phase stability of alloy *A*, calculated with ThermoCalc¹⁵

Slika 4: Teoretična ravnotežna termodinamska stabilnost faz zlitine *A*, izračunana z orodjem ThermoCalc¹⁵

fore, only the main results will be presented. The thermodynamic analysis of alloy *B* shows⁹ that the alloy in equilibrium mostly contains the solid crystals of the α Al phase (from room temperature up to 562.64 °C), the crystals of Si (up to 619.72 °C) and the intermetallic phases of Al₂Cu (up to 447.85 °C) and Al₅Cu₂Mg₈Si₆ (up to 526.04 °C). The first liquid is formed at 532.65 °C. This alloy does not have a two-phase L + α Al region because of a high amount of Si and its high temperature stability. Therefore, there is only the three-phase L + α Al + Si temperature region (between 532.65 °C and 562.65 °C) appropriate for the liquid-phase sintering. The powder producer recommends the sintering temperatures between 540 °C and 560 °C for 60 min, which is again in good agreement with the theoretical calculations. A longer sintering time may be prescribed to the low solubility of Si.

The thermodynamic analysis of alloy *C* shows⁹ that, in equilibrium, this alloy mostly contains the solid crystals of the α Al phase (from room temperature up to 630 °C) and intermetallic phases of Mg₂X₂C₁ (X = Sn, up to 511.13 °C), S₂Al₂CuMg (up to 442.70 °C), MgZn₂ (up to 409.71 °C) and T₁AlCuMgZn (up to approximately 250 °C). The first liquid is formed at 516.54 °C. A two-phase region (L + α Al) exists between 516.54 and 630 °C. This temperature region is relatively wide. At the beginning of this temperature region (somewhere between 530 °C and 560 °C) where a small amount of liquid is already formed, there is the appropriate optimum sintering temperature predicted by ThermoCalc. However, the powder producer recommends a higher sintering temperature (between 600 °C and 610 °C for 20 min), which is still in agreement with the theoretical calculation. A higher sintering temperature is possible with a slightly shorter sintering time (for example, 15 min instead of 20 min). But, there is always the issue of the final optimization of the sintering process that is, unfortunately, still primarily based on the experimental work.

From the thermodynamic analyses of the selected alloys it is also clear that after the sintering (designated as T1a) all three alloys can be additionally heat treated with the conventional standardized precipitation-strengthening (also age-hardening) procedure, i.e., solid-solution annealing combined with fast cooling (quenching) and natural (T4) or artificial ageing (T6, T76, etc.). In this case the temperature of solid-solution annealing must be below the formation temperature of the first liquid in the region of the maximum solid solubility of the alloying elements in Al, typically 500 °C for 20 min. After homogenization very fast cooling must be performed, enabling a formation of a supersaturated solid solution of the α Al phase with the alloying elements. The final step of the heat treatment is natural (ambient conditions) or artificial (at an elevated temperature) ageing, typically 150 °C for 15 min. A precipitation of a very fine dispersion of intermetallic phases

occurs during this step. An ageing temperature that lasts for too long and is too high can cause an unwanted growth of the precipitates decreasing the hardness and strength of the alloy. As in the case of sintering, the final optimization of the age-hardening process is unfortunately still based on the expensive and time-consuming experimental work. However, new computer tools^{13–15} calculating theoretical CCT (continuous cooling temperature) and isothermal TTT (time-temperature transformation) diagrams can significantly reduce the experimental work. At the cooling rate of 10^5 °C/h (approximately 28 °C/s) a fine precipitation of GP (Guiner-Preston) zones and the theta prime (θ') phase are predicted.⁹ In the case of lower cooling rates other (unwanted) intermetallic phases would also develop.

Figure 5 shows the theoretical thermodynamic phase stability in the system with the chemical composition of the SB powder. One can see that in this system, depending on the temperature, there can be eleven (11) phases, compared to only seven (7) in alloy *A*, five (5) in alloy *B* and six (6) in alloy *C*. The liquid and α Al are stable together in the temperature region between approximately 527 °C and 617 °C. However, besides α Al the most temperature-stable solid phases in this system are Al_6Mn and Alfa (Al-Fe-Mn-Si-Cu) that are still solid above 645 °C and 609 °C, respectively. For the optimum liquid-phase sintering conditions it would be recommendable that these two phases are also dissolved in the α Al solid solution. Unfortunately, in this alloying system a two-phase region (α Al + L) does not exist and the optimum sintering conditions cannot be assured.

This theoretical thermodynamic analysis shows that commercial Al powders have designed chemical compositions that enable reactive liquid-phase sintering. However, the SB powder has a more complex chemical composition that is not accommodated for the optimum sintering process. By analogy with the determination of the sintering temperatures of the commercial Al powders

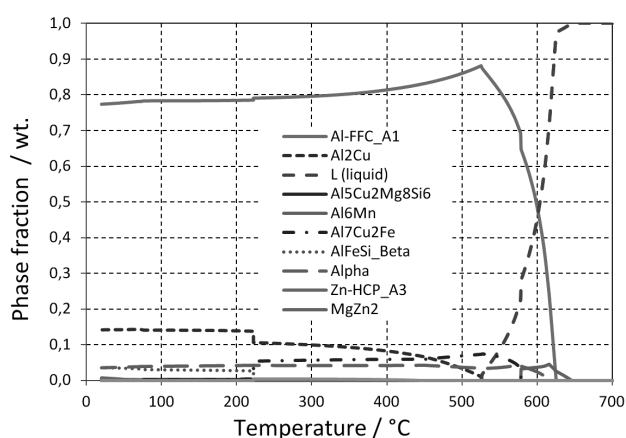


Figure 5: Theoretical equilibrium thermodynamic phase stability of the alloy with the SB-powder composition, calculated with ThermoCalc¹⁵

Slika 5: Teoretična ravnotežna termodinamska stabilnost faz v sistemu s kemično sestavo SB-prahu, izračunana z orodjem ThermoCalc¹⁵

(approximately 10 % to 20 % of the liquid phase present), the optimum sintering temperature of the SB powder is somewhere between 550 °C and 590 °C. But in this temperature region, besides the liquid and α Al, there is still a relatively large amount of the intermetallic phases of AlFeSi-Beta, Al_6Mn and Alpha. All these intermetallic phases are only dissolved in the liquid phase above 645 °C, but then the α Al phase also completely disappears, i.e. only the liquid phase is present and complete melting of the material occurs. On the other hand, it is necessary to know that the sinterability of a metal powder does not depend only on the chemical composition and thermodynamic conditions but also on the other parameters (particle-surface oxidation, particle shape and size, homogeneity of the powder mixture, sintering atmosphere, etc.) that control the sintering kinetics and cannot be fully covered in this theoretical study.

3 MORPHOLOGICAL CHARACTERISTICS OF THE POWDERS

For a successful industrial mass production of small complex parts, besides a good final densification of a powder compact with sintering, the preceding processing step, i.e., the automatic uniaxial cold or warm die compaction (ADC) in the metal mould with automatic mechanical or hydraulic presses is also important. The selected metal powder must flow fast and continuously from the powder container through the filling tube and the shoe into the die cavity, where it is fast compacted with as low as possible pressure into a green compact with a high green density and strength, as well as without any internal or surface defects (cracks, flaws). The powder must completely fill all the parts of the die cavity. For this reason, besides a suitable chemistry, the metal powder must also have an appropriate particle morphology (the size distribution and shape). This is mainly controlled with the powder production process (atomisation, milling, powder heat treatment, etc.). Several standardized tests and investigations make it possible to evaluate the usability of the powder mixture for an ADC process and its technological properties.¹⁶ The most important are the apparent and tap densities, the flowability and compressibility that are controlled with the particle morphology, as well as chemical and metallurgical conditions of a powder production. For example, the results of an atomization¹⁷ are hard particles generally formed during fast cooling of the droplets of a melt; a mixture of pure soft elemental and hard alloyed particles gives a better compressibility than a prealloyed, chemically uniform powder, etc. The type and amount (1 % to 2 %) of a lubricant influence, to some extent, the technological properties of a powder mixture. The apparent density and flowability of a powder are determined with a Hall flowmeter.¹⁶ Through a funnel of a standardized size, 50 g or 100 g of powder flows for a defined period. The flow time is measured (for example,

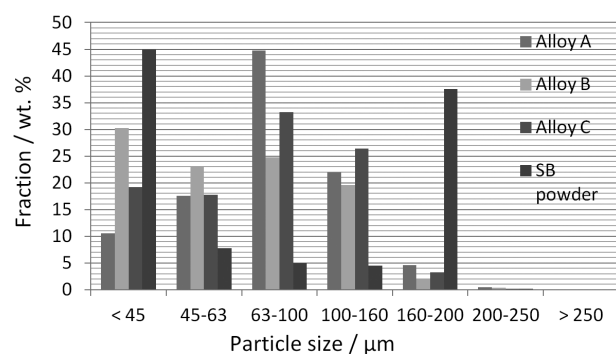
Table 2: Main technological properties of the investigated Al powders important for the ADC process**Tabela 2:** Glavne tehnološke lastnosti izbranih Al-prahov, pomembne za uspešno avtomatsko hladno enoosno stiskanje v surove končne oblike izdelka

Property	Powder type	Alloy A	Alloy B	Alloy C	SB powder
Apparent density (g/cm ³)	nominal ¹⁰	1.05–1.15	1.05–1.25	1.1–1.25	n. d.
	actual	1.08	1.12	1.14	1.20
Tap density (g/cm ³)	nominal ¹⁰	1.2–1.5	1.2–1.5	1.2–1.5	n. d.
	actual	1.32	n. d.	n. d.	1.25
Flowability (seconds/50g)	nominal ¹⁰	< 30	n. d.	< 30	n. d.
	actual	24	n. d.	n. d.	not flowable
Green density (g/cm ³)	nominal ¹⁰	2.65 at 400 MPa	2.56 at 620 MPa	2.65 at 400 MPa	not defined
	actual	2.68 at 440 MPa	2.52 at 600 MPa	2.61 at 430 MPa	2.37 at 516 MPa
Fine fraction (< 45 μm), w/%	max. 20	25–40	max. 35		45

(30 s)/(50 g)) and the value is designated as the powder flowability. At the same time this powder is collected in a small copper pot with a known volume (25 cm³), weigh and apparent density of the loose powder, calculated in g/cm³ (typically approximately 3 g/cm³ for the Fe- and 1.2 g/cm³ for the Al-based powders). The loose powder is generally densified, to some extent, with mechanical vibration. The tap density is a result of 100 mechanical vibrations of the loose powder. The compressibility of a powder is determined with a standardized tool measuring the mechanical pressure needed for a certain green density of a compact (typically approximately 600 MPa for the green density of 7.0 g/cm³ of a steel-powder compact and 400 MPa for the green density of 2.6 g/cm³ of an Al-powder compact, respectively).¹⁷

Table 2 shows the main technological properties of the investigated powders. It can be clearly noticed that the commercial powders have smaller parts of the fine fraction of powder particles, better flowability and compressibility than the SB powder.

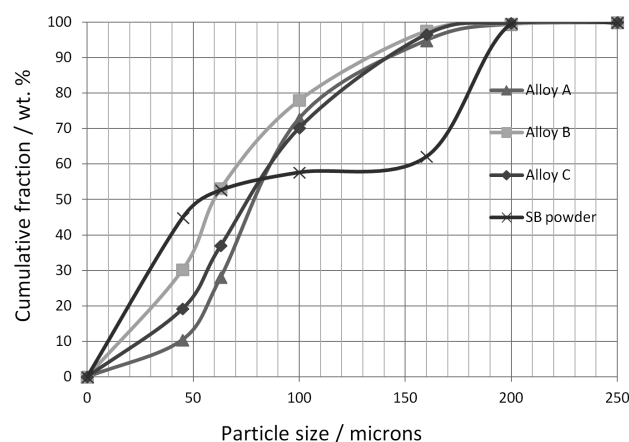
Figures 6 and **7** show the results of the complete sieving analyses of the investigated powders. The SB powder mainly consists of two fractions. The fine < 45 μm fraction is a result of the sand blasting of discs and slugs, i.e., small-scale particles (worn parts), and the coarse-particle fraction of 160–200 μm is a result of the

**Figure 6:** Particle-size-distribution histogram of the investigated Al-based powders based on the performed sieving analyses**Slika 6:** Histogram velikostne porazdelitve delcev preiskovanih prahov, izdelan na osnovi sejnalne analize

incompletely worn sand-blasting media. On the other hand, the commercial Al powders have a relatively uniform natural-particle-size distribution with a regular *S* curve of the cumulative-particle-size distribution (**Figure 7**). The SB powder also has a lower mean particle size; as observed from the *S* curve, *d*₅₀ is approximately 53 μm for the SB powder in comparison with alloys A (80 μm), B (60 μm) and C (78 μm).

4 MICROSTRUCTURAL CHARACTERISTICS OF THE POWDERS

The revealed technological properties of the investigated powders are the results of their micromorphological and microchemical characteristics. The microstructural and microchemical investigations of the powders performed with LM and SEM/EDS are shown below. The observations under the microscopes were performed in a loose condition (powder particles stacked on a special tape), as well as in cross-section (polished and etched metallographic samples). **Figures 8** and **9** show the SEM micrographs of loose powders A and B at two different magnifications. Powder C has a similar particle morphology.

**Figure 7:** Cumulative-particle-size distribution of the investigated Al-based powders based on the performed sieving analyses**Slika 7:** Kumulativne velikostne porazdelitve delcev preiskovanih prahov, izdelane na osnovi sejnalne analize

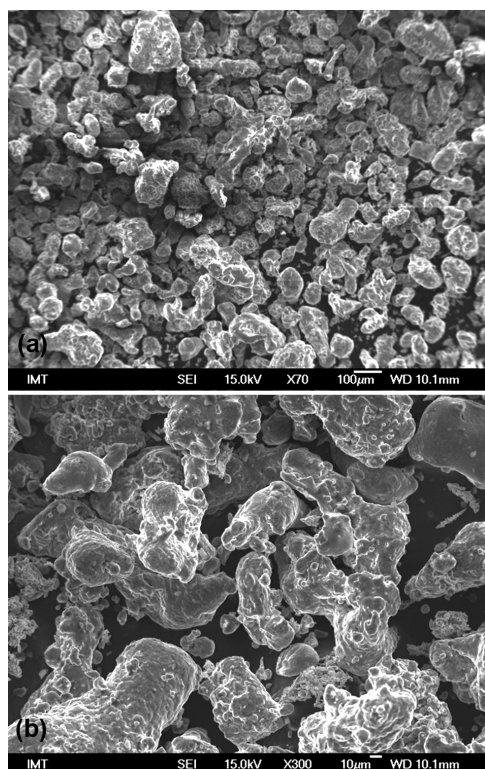


Figure 8: SEI micrographs of loose powder A made at two different magnifications

Slika 8: SEI-posnetka nasutega prahu A, narejena pri dveh različnih povečavah

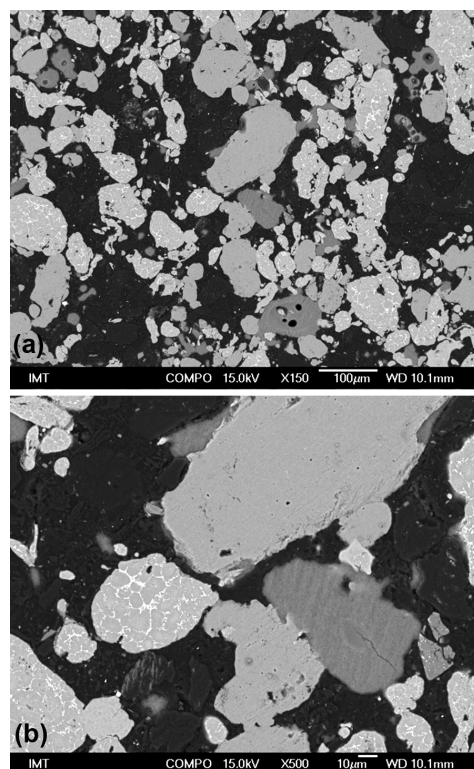


Figure 10: SEM/BEI micrographs of powder B in cross-section, made at two different magnifications

Slika 10: SEM/BEI-posnetka nasutega prahu B v prerezu, narejena pri dveh različnih povečavah v povratno sipanih elektronih

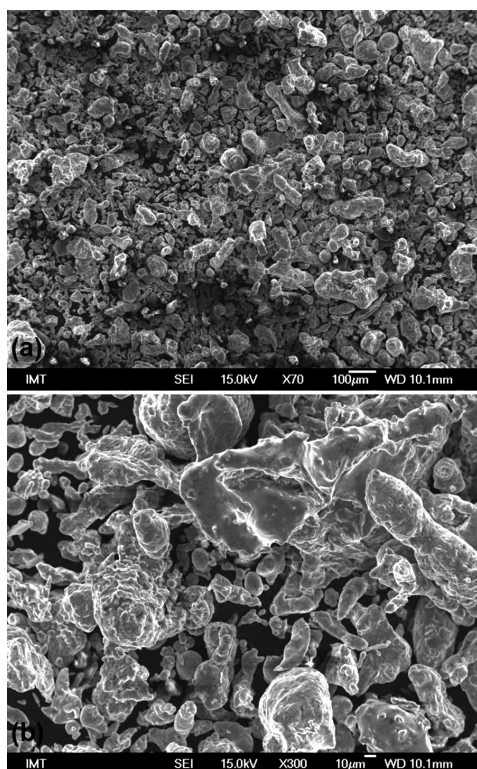


Figure 9: SEI micrographs of loose powder B made at two different magnifications

Slika 9: SEI-posnetka nasutega prahu B, narejena pri dveh različnih povečavah

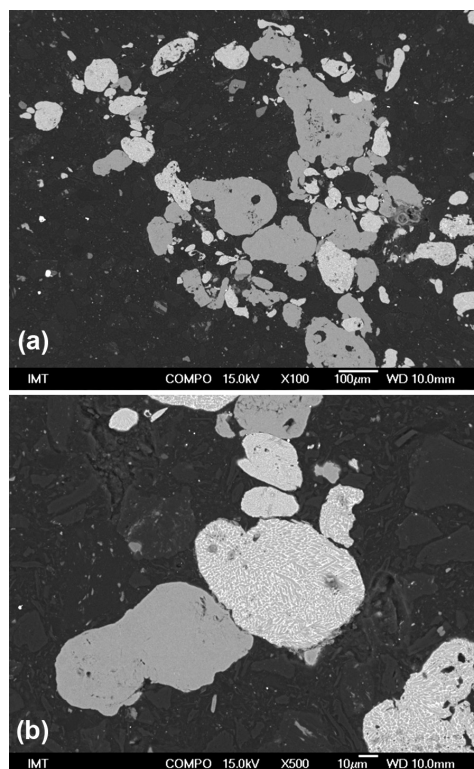


Figure 11: SEM/BEI micrographs of powder C in cross-section, made at two different magnifications

Slika 11: SEM/BEI-posnetka nasutega prahu C v prerezu, narejena pri dveh različnih povečavah v povratno sipanih elektronih

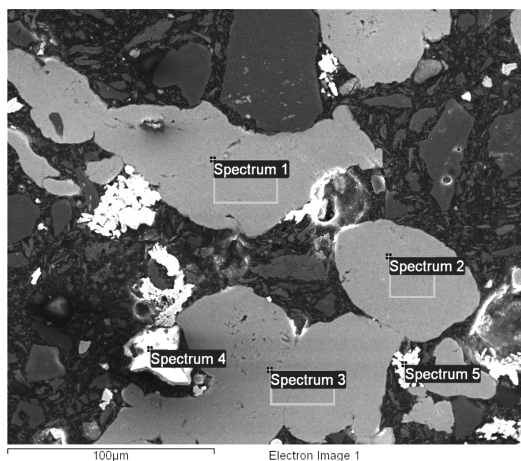


Figure 12: SEM/BEI micrograph of individual particles of powder A in cross-section where the EDS microanalysis was performed

Slika 12: Posnetek mest na posameznih delcih prahu A, kjer je bila izvedena SEM/EDS-mikroanaliza

It can be seen that the commercial powders have irregular particle shapes (rounded droplets) with smooth vitreous surfaces and different sizes from approximately 1 µm to 200 µm. This particle morphology is typical for gas (air) atomized Al powders.

Figures 10 and 11 show the SEM/BEI (backscatter electron image mode) micrographs of the powder particles of alloys B and C in cross-section at two different

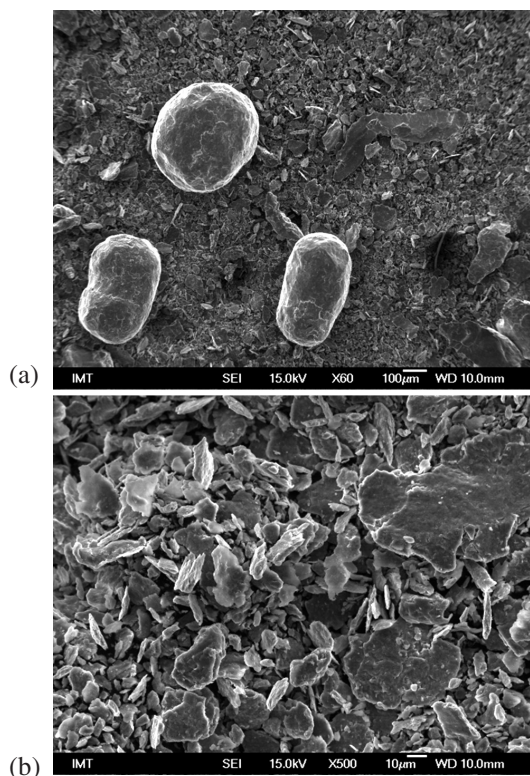


Figure 13: SEI micrographs of the loose SB powder, made at two different magnifications

Slika 13: SEI-posnetka kovinskega SB-prahu, narejena pri dveh različnih povečavah

magnifications. In both powders it can be clearly seen that the particles are of different colours (shades of grey). This means that they have different chemical compositions. It can also be seen that small white irregular shapes are present in powder A. The microchemistry of the powders was checked with the SEM/EDS microanalyses of individual powder particles.

It has been shown that all the commercial powders consist of the powder particles with different chemical compositions. In the case of powder A (**Figure 12** and **Table 3**), the powder mixture contains the particles of pure soft Al, the Al-Si alloy (approximately 90 % Al and 10 % Si) and the Cu-Al alloy (approximately 95 % Cu and 5 % Al). It is also confirmed that the small white clusters of particles are oxides (mainly SiO₂, some Al₂O₃ and CaO).

The SEM/EDS analysis of some particles of powder B has shown that this powder is also a powder mixture of pure Al as well as the alloyed particles of Al-Si-Mg-Cu and Si-Al. All the particles are considerably surface oxidized. Powder C is a mixture of pure Al particles and the alloyed particles with the approximate composition of Al-12Zn-5Mg-4Cu. This powder is the least oxidized of all the commercial powders.

Figures 13a and **13b** show SEM micrographs of the loose SB powder at two different magnifications. In **Figure 13a**, made at a lower magnification, large round particles of the sand-blasting media are clearly visible. However, at larger magnifications (**Figure 13b**) we clearly see small irregular particles (scales or shells) formed due to the sand blasting of discs and slugs. The SB powder has a low flowability and compressibility because of its particle morphology.

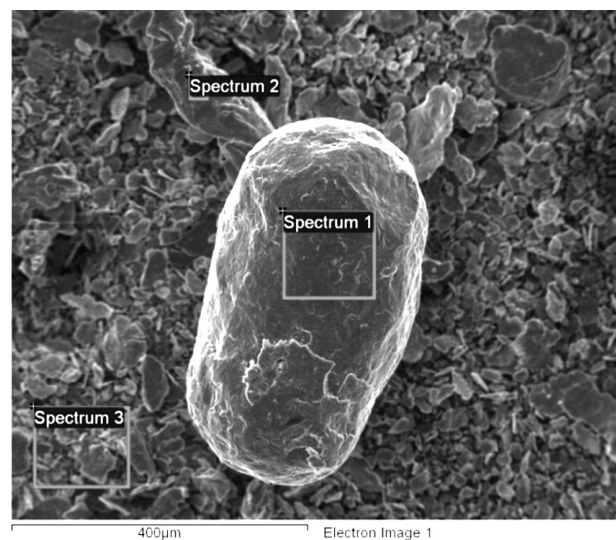


Figure 14: SEM/EDS analysis of a larger spherical particle and smaller-scale particles with designated locations of the performed analyses (connected with **Table 4**)

Slika 14: SEM/EDS-analiza večjih sferičnih in manjših luskinastih delcev z označenimi mesti izvršene analize in tabelarično podanimi rezultati analize delcev (**tabela 4**)

Table 3: Microchemical compositions of individual powder particles of powder mixture A (connected with **Figure 12**)

Tabela 3: Mikrokemijska sestava posameznih delcev prašne mešanice A (vezano na **sliko 12**)

Spectrum	O	Al	Si	Ca	Cu	Total
Spectrum 1		100.00				100.00
Spectrum 2		89.32	10.68			100.00
Spectrum 3		100.00				100.00
Spectrum 4	55.69	2.28	41.04	0.98		100.00
Spectrum 5		5.45			94.55	100.00

Figure 14 shows the SEM/EDS analysis of a larger spherical particle (Spectrum 1) in the region where small-scale particles are also present (Spectrum 3). As it can be seen in **Table 4**, the large spherical particle is surface oxidized and, besides Al, it also contains Si, Mn, Fe, Cu and Zn, which is in accordance with the chemical analysis of the sand-blasting media (**Table 5**). However, the larger flat particle is practically pure Al (Spectrum 2) but also surface oxidized.

Table 4: Microchemical compositions of individual powder particles of the SB powder (connected with **Figure 14**), w/%

Tabela 4: Mikrokemijska sestava posameznih delcev SB-prahu (vezano na **sliko 14**), w/%

Spectrum	O	Al	Si	Mn	Fe	Cu	Zn	Ag
Spectrum 1	17.11	74.39	0.77	0.27	0.94	4.97	1.14	0.41
Spectrum 2	4.12	95.88						
Spectrum 3	15.29	76.29	0.66		1.02	5.59	1.16	

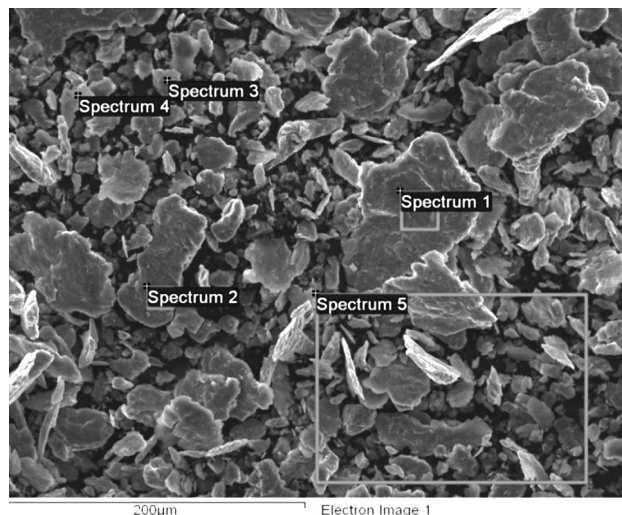


Figure 15: SEM/EDS analysis of smaller-scale particles with designated locations of the performed microanalyses (connected with **Table 6**)

Slika 15: SEM/EDS-analiza manjših luskinastih delcev z označenimi področji, kjer je bila izvršena analiza (v povezavi s **tabelo 6**)

Table 5: Chemical composition and properties of the sand-blasting media

Tabela 5: Kemijska sestava in lastnosti peskalnega sredstva

Element	Si	Mn	Fe	Cu	Zn	Pb	Mg	Particle size (µm)	Apparent density (g/cm ³)	Hardness HV _{0.2}
Composition (w/%)	0.6–1.2	0.3–0.6	1.0–1.5	6.0–6.5	1.0–1.5	< 0.15	< 0.3	150–400	1.65	90–120

Figure 15 and **Table 6** show the results of SEM/EDS analyses of the regions where mainly fine particles are present. Fine-scale particles are substantially surface oxidized and, as a result of the sand blasting, they contain all the elements present in discs and slugs as well as in the residuals of the sand-blasting media.

Table 6: Microchemical compositions of individual fine-powder particles of the SB powder (connected with **Figure 20**), w/%

Tabela 6: Mikrokemijska sestava posameznih finih delcev SB-prahu (vezano na **sliko 20**), w/%

Spectrum	O	Al	Si	Mn	Fe	Cu	Zn	Ag
Spectrum 1	16.62	75.76	0.93	0.39	0.92	4.51	0.87	
Spectrum 2	13.86	77.85	0.89	0.33	1.16	4.71	0.75	0.46
Spectrum 3	17.45	74.87	1.37		0.89	4.51	0.92	
Spectrum 4	9.70	82.49	1.07		0.94	4.42	0.93	0.44
Spectrum 5	15.45	76.02	0.79	0.47	1.17	5.16	0.95	

5 COMPACTION AND SINTERING OF THE POWDERS

The investigated commercial powders were compacted into standard^{11,16,17} tensile-test specimens (35 pieces

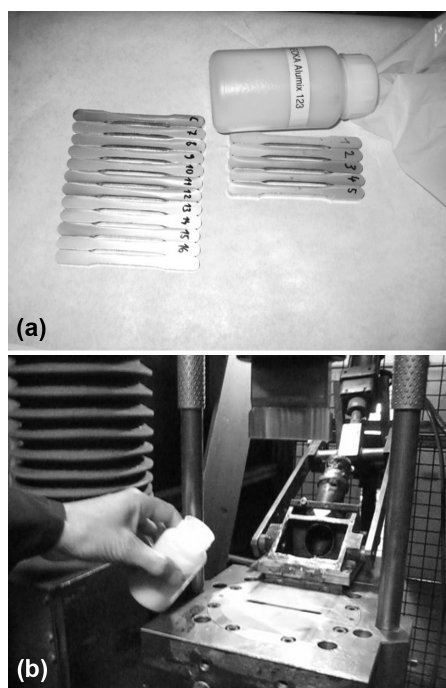


Figure 16: Powder-compaction experiments: a) standardized tensile-test specimens compacted from Al-based commercial powders and b) manual pouring of the powder into a die cavity

Slika 16: Preizkusi stiskanja prahov: a) standardni natezni preizkušanci, stisnjeni iz komercialnih Al-prahov in b) ročno nasipanje Al-prahu v orodje

of each powder, **Figure 16a**) with a 60 MN Dorst mechanical press, Germany, in the Unior factory, Zreče. The powders were manually dosed (poured) into the die cavity (**Figure 16b**). Powders *A* and *C* were compacted at approximately 450 MPa. Powder *B* has a lower compressibility and was, therefore, compacted at approximately 600 MPa. The corresponding average green densities are given in **Table 7**. The samples were then sintered in a batch lab furnace under the prescribed sintering conditions. The obtained average sintered densities and mechanical properties are also given in **Table 7** and they are in accordance with the expectations (the nominal values for the T4 condition are given in parentheses). As a case study, the LM micrographs of the green and sintered compacts of powder *B* are given in **Figures 17a** and **17b**. It is well visible that the remaining porosity of the green compact after cold compaction is still relatively large. However, after the sintering a good

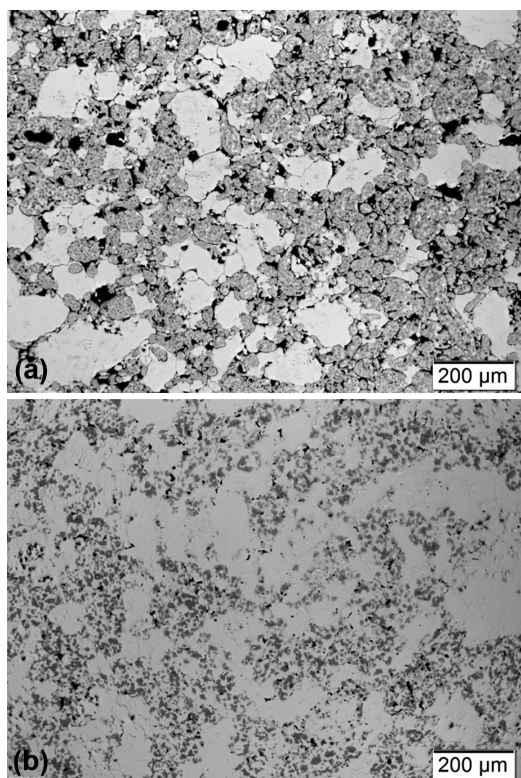


Figure 17: Microstructure of powder *B*: a) after cold compaction and b) after sintering, visible under a light microscope

Slika 17: Mikrostruktura vzorca iz prahu *B*, vidna pod svetlobnim mikroskopom: a) po hladnem stiskanju in b) po sintranju

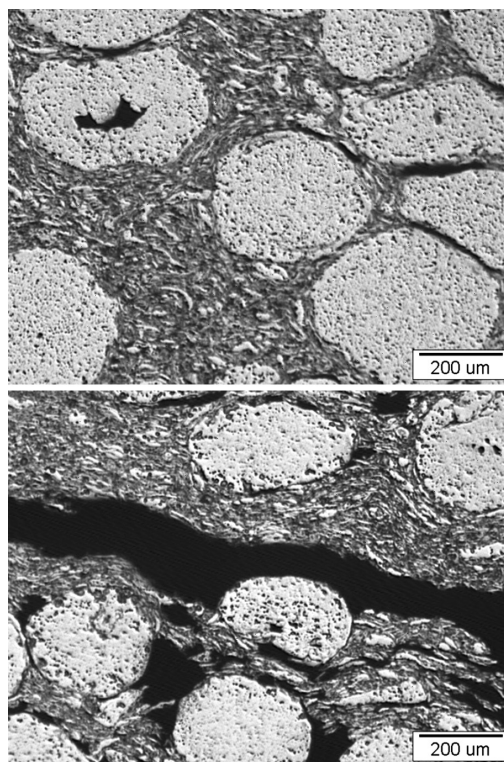


Figure 18: Microstructure of the SB powder after sintering with a well visible, irregular particle morphology and local defects (pores, lunkers and flaws)

Slika 18: Mikrostruktura sintranega SB-prahu, vidna pod svetlobnim mikroskopom z dobro vidno neregularno morfologijo delcev in lokalnimi napakami (pore, lunckerji in plastne razpoke)

densification is obtained and only a small amount of residual porosity remains. One can also notice that the compacted powder mixture mainly consists of two types of particles (pure Al and alloyed particles of Al-Si-Mg-Cu), which was also confirmed with SEM/EDS analyses. This chemical inhomogeneity with the traces of a different initial-particle composition also remained after the sintering.

The SB powder was also experimentally compressed and sintered. However, because of its low compressibility observed already in the case of green compacts, at high compaction pressures (at 520–620 MPa only 2.25–2.37 g/cm³) flaws are formed. The sinterability of the powder is also low; therefore, a low sintering density was obtained together with a high porosity and a significant amount of different defects (**Figure 18**).

Table 7: Results of the compaction and sintering of the tensile-test specimens of commercial Al-based powders (average values)

Tabela 7: Rezultati stiskanja in sintranja epruвет iz preiskovanih Al-prahov (povprečne vrednosti)

Powder designation	Green density	Sintered density	Hardness HB _{2.5/31.25}	Tensile strength	Yield strength	Module of elasticity	Elongation at fracture
	g/cm ³						
Alloy A	2.62	2.60	65 (60)	202 (190)	156	3834	2.23 (5)
Alloy B	2.52	2.62	104 (100)	239 (200)	219	4399	0.70 (1)
Alloy C	2.61	2.73	102 (100)	325 (270)	250	4102	3.90 (5)

Our morphological and microstructural investigations confirmed that the SB powder has an inappropriate chemical and particle morphology. It would have to have more suitable morphological properties in order to be appropriate for the use in conventional ADC and sintering technology. Firstly, the flowability and compressibility of the powder have to be improved. This could be achieved by adding an appropriate amount (approximately 50 % to 60 %) of soft, commercially available, pure Al powder (> 99.8 % of Al) with a suitable particle shape and size distribution. An additional procedure should be a removal of the remaining coarse particles of the sand-blasting media with 180 µm or 250 µm sieves. The sand-blasting media contains relatively large amounts of Fe, Mn and Zn, and sieving would probably significantly decrease the amounts of these elements in the SB powder. However, the correct chemical composition similar to that of the standardized Al-Cu-Si-Mg alloy (for example, type 2xxx) would still not be attained and additional corrections of the chemical composition would be necessary. In spite of this, the final target composition will be very difficult to obtain completely. Therefore, it seems that SB powder can be more suitable for the production of selected dispersion-strengthening alloys.

6 USE OF SB POWDER FOR DISPERSION STRENGTHENING

SB powder is a relatively good raw material with approximately 86 % to 87 % of Al. But it also contains a significant amount of oxides. Therefore, it seems that SB powder is more usable for the production of Al/Al₂O₃

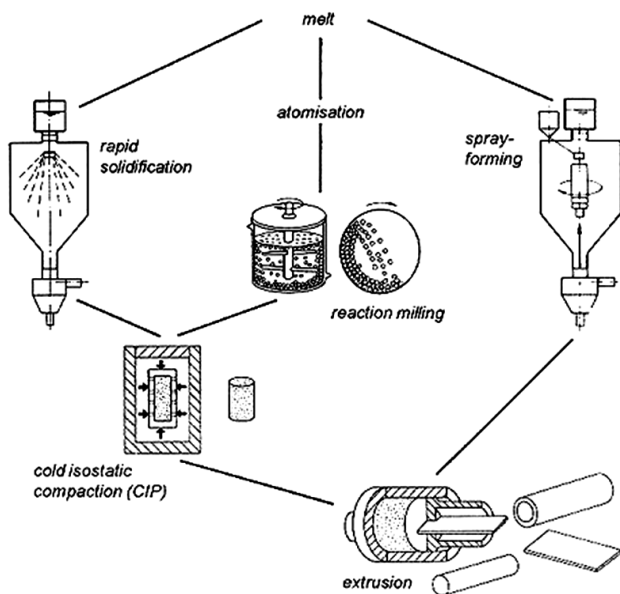


Figure 19: Three different but related P/M technologies for the production of high-strength, thermally stable ODS Al-based alloys¹⁷

Slika 19: Trije različni, toda sorodni P/M-postopki izdelave visoko trdnih disperzijsko utrjenih Al-zlitin¹⁷

composites using the modified oxygen-dispersion-strengthening (ODS) technology than for conventional sintering technology. The technology of preparing ODS alloys was started already in the early 1950s by A. V. Zeerlender and R. Irrmann.^{11,17} As a matter of fact, it was originally developed for the use of the Al scrap containing a lot of metallic oxides. The appropriate powder mixture for the initial sintering (sintered aluminium powder, SAP) was obtained by grinding and milling the scrap and the end result was a semi-final or final extruded or forged composite with the oxide-particle size of 10 µm to 100 µm. However, later a lot of modifications and improvements of the technology were introduced using atomized powders and high-energy reaction ball milling (**Figure 19**). In this way various Al-based composites with a fine micro/nano dispersion of complex oxides, nitrides and borides can be formed, such as Al/Me_xO_y (for example, Al₂O₃), Al/M_xC_y (Al₄C₃, SiC), Al/M_xN_y (BN, TiN, ZrN, TiB₂, etc.) or their combinations. Nowadays, high-quality Fe- and Ni-based ODS superalloys with a fine dispersion of thermally stable oxides (Y₂O₃) or intermetallics are also produced.

In our case, to use the SB powder only the last steps (high-energy reaction ball milling, CIP and warm/hot extrusion) given in **Figure 19** could be used and some additional steps (initial sieving of the powder, pre-sintering of CIP preforms) would have to be introduced. Fine Al powders are very reactive and very dangerous with respect to self-ignition and explosion, therefore, a highly inert protective atmosphere has to be used.¹⁸ A modification of this procedure would also be useful for the production of Al foams introducing the foaming reagents such as TiH₂ or CaCO₃.¹⁹ This process is very complex, but it generally gives an excellent microstructure with good mechanical properties and a thermal stability of the material. However, a lot of technical and market-related questions remain to be solved in the frame of a new project introducing this technology using SB powder.

7 CONCLUSIONS

In the frame of our investigations, practical usability of the Al powder formed as a bypass product of the sand blasting of slugs and discs was analysed. The so-called SB powder was compared with commercially available Al-based powders used for conventional sintering technology. Our theoretical thermodynamic analyses as well as morphological and microstructural investigations have shown that the investigated Al powder has inappropriate chemical and particle morphologies for conventional sintering technology. It seems that it is a much more suitable raw material for the production of Al/Al₂O₃ composites using modified ODS technology. This still has to be confirmed in the frame of a new, additional experimental research.

Acknowledgement

Authors wish to thank to the Slovenian Research Agency for the financial support in the frame of the project No. L2-4283, as well as the powder producer of Ecka Granules, Germany, and the Unior Forging Industry, Zreče, for their assistance with the experiments.

8 REFERENCES

- ¹ R. M. German, Powder Metallurgy Science, Metal Powder Industries Federation (MPIF), 1st and 2nd edition, Princeton, New Jersey 1984, 1994
- ² M. J. F. Gándara, Aluminium, The metal of choice, Mater. Tehnol., 47 (2013) 3, 261–265
- ³ P. Lichý, M. Cagala, J. Beňo, Investigation of the thermomechanical properties and microstructure of special magnesium alloys, Mater. Tehnol., 47 (2013) 4, 503–506
- ⁴ Indiamart, web pages: <http://sourcing.indiamart.com/engineering/articles/aluminum-gears/> and <http://dir.indiamart.com/cgi/catprd-search.mp?ss=aluminium+gears>
- ⁵ Aluminium Powder Metallurgy, web page: <http://www.aluminum.org/Content/NavigationMenu-/The-Industry/PowderandPaste/PowderMetallurgy.PDF>, Al Association Inc.
- ⁶ Powder Metallurgy of Al and Al alloys, Powder Metal Technologies and Applications, Vol. 7, ASM Handbooks
- ⁷ B. Šuštaršič, J. Medved, S. Glodež, M. Šori, A. Korošec, DSC/TG of Al-based Alloyed Powders for P/M Applications, Presentation at 21st international conference on Materials and Technology, Portorož, Slovenia, 2013
- ⁸ Talum, Factory of Aluminium, Kidričevo, Slovenia, web page: <http://www.talum.si/en/slugs>
- ⁹ B. Šuštaršič, I. Paulin, M. Godec, S. Glodež, M. Šori, J. Flašker, A. Korošec, Morphological and microstructural features of Al-based powders appropriate for P/M applications, University of Maribor, Slovenian Research Agency, project L2-4283 (2012–2014), phase report (in Slovenian language) and oral presentation at 21st international conference on Materials and Technology, Portorož, Slovenia, 2013
- ¹⁰ ECKA Granules, web page: <http://www.ecka-granules.com/en/ecka-granules/products/>
- ¹¹ E. A. Brandes, G. B. Brook, Smithells Metals Reference Book, 7th edition, Butterworth Heinemann, Oxford, UK 1992
- ¹² ASM Alloy Phase Diagram Database, P. Villars, editor-in-chief, H. Okamoto and K. Cenzual, section editors, ASM International, Materials Park, OH, 44073, USA, 2006–2013
- ¹³ U. R. Kattner, Thermodynamic Modeling of Multicomponent Phase Equilibria, JOM, 49 (1997) 12, 14–19
- ¹⁴ J. F. Chinella, Z. Guo, Computational Thermodynamics Characterization of 7075, 7039, and 7020 Aluminum Alloys Using JMatPro, ARL-TR-5660, USA, 2011
- ¹⁵ Thermocalc, web page: <http://www.thermocalc.com/>, software package for thermodynamic calculations
- ¹⁶ Metal Powder Industries Federation, web page: <http://www.mpif.org/>
- ¹⁷ Powder Metallurgy CD, Materials Processes and Applications, Leonardo project, EPMA Education Working Group, 2001
- ¹⁸ General Safety Recommendations for storage and handling of Al powder and pastes, http://www.aluminum.org/Content/NavigationMenu/TheIndustry/PowderandPaste/TR2_2006.pdf
- ¹⁹ I. Paulin, Synthesis and characterisation of Al foams, Ph. D. thesis, Ljubljana, 2011